

Efficient finite-difference method for quasi-periodic steady-state and small signal analyses

Baolin Yang
Cadence, San Jose, CA
byang@cadence.com

Dan Feng
Cadence, San Jose, CA
feng@cadence.com

ABSTRACT

This paper discusses a finite-difference mixed frequency-time (MFT) method for the quasi-periodic steady-state analysis and introduces the quasi-periodic small signal analysis. A new approach for solving the huge nonlinear system the MFT finite difference method generates from practical circuits is given, which makes efficient frequency-sweeping quasi-periodic small-signal analysis possible. The new efficient solving technique works well with the Krylov-subspace recycling or reuse [4], which can not be achieved with existing techniques. In addition, this paper gives a way to calculate the quasi-periodic Fourier integration weights, necessary in the adjoint MFT small-signal analyses, and a way to calculate quasi-periodic large-signal Fourier spectrum that is more efficient than existing methods. Numerical examples also show that the finite-difference MFT method can be significantly more accurate than shooting-Newton MFT method and the new preconditioning technique is more efficient.

1. INTRODUCTION

The exploding demand for high performance wireless products has increased the need for efficient and accurate simulation techniques for RF integrated circuits. RF circuit simulation is difficult because RF circuits typically contain signals with multiple-timescale properties, as usually the data and carrier signals in a system are separated in frequency by several orders of magnitude. The situation is further complicated by the fact that many multi-timescale circuits have a response (mixers and switched-capacitor filters are good examples) that is highly nonlinear with respect to at least one of the exciting inputs, and so steady-state approaches such as multi-frequency harmonic balance do not perform well.

To circumvent these difficulties, mixed frequency-time approaches (MFT) have been proposed and an efficient implementation based on shooting method has been given [1] for obtaining quasi-periodic steady-state of practical circuits. In the MFT approach, we use time-domain method to resolve the strongly nonlinear tone and frequency-domain method to resolve the weakly nonlinear tone present in the circuit. Thus the advantage of both time-domain method and frequency-domain method is utilized. This method can be extended

to quasi-periodic small signal analyses with the same advantage. Several difficulties need to be resolved in this extension.

First, the large-signal MFT method in [1] uses a nested-GMRES matrix-implicit iterative solver which can not be used efficiently with Krylov-subspace recycling or reuse technique to do a multi-frequency small-signal analysis sweep. As Krylov-subspace recycling is crucial for the efficiency of small signal analyses, a new matrix-implicit iterative formulation that can be used efficiently with Krylov-subspace recycling needs to be devised. Second, in small signal analyses such as noise analysis, one often uses the adjoint analysis. Adjoint analysis is the transpose of $c \cdot Y^{-1}(s)u^T$, where $Y^{-1}(s)$ is the Jacobian matrix of the circuit equation and c is the Fourier integration coefficients for spectrum calculation. The Fourier spectrum operator ($c \cdot$) can be done in several steps with the explicit form of c unknown. Existing MFT techniques perform the quasi-periodic Fourier spectrum analysis in several separate steps and c is not calculated. For adjoint analysis, we need to compute $u \cdot (Y^{-1}(s))^T c$ where the coefficient vector c must be given explicitly, a non-obvious task for the quasi-periodic MFT method. Last, small signal analyses typically uses a finite-difference method for discretization while the MFT method in [1] uses the shooting method as the discretization method.

In this work, we first present a finite difference MFT method for quasi-periodic large signal analysis. Then we discuss the quasi-periodic MFT small-signal analyses, using the quasi-periodic steady state as the operating point of the circuit. Small signal analyses allow us to calculate important circuit parameters such as transfer function and noise figure. These analyses are typically swept for a range of frequencies. To efficiently solve this multi-frequency problem, a new matrix-free efficient iterative formulation for the MFT finite difference method, successfully used with Krylov-subspace recycling techniques for small signal analyses, is presented. It allows us to sweep a large number of frequencies at a cost of a few. This new method is simpler in formulation and more suitable for the application of time-domain high-order methods such as that given in [2]. In the end, we give an efficient way to obtain the quasi-periodic Fourier integration weights needed in the small signal analyses. The approach can also be applied efficiently in calculating the Fourier spectrum of the quasi-periodic steady-state solution.

Using the efficient matrix-implicit Krylov-subspace techniques, we can simulate large circuits with non-commensurate large-signal tones of which one can be very nonlinear and calculate the noise parameters of such circuits. The small signal analyses after the quasi-periodic large signal analysis are usually more interesting to circuit

designers than the large signal analysis itself.

2. BACKGROUND ON THE MFT APPROACH

Circuit behavior is usually described by a set of nonlinear differential-algebraic equations (DAEs) that can be written as

$$\frac{d}{dt}Q(v(t)) + I(v(t)) + u(t) = 0,$$

where $Q(v(t)) \in \mathfrak{R}^N$ is typically the vector of sums of capacitor charges at each node, $I(v(t)) \in \mathfrak{R}^N$ is the vector of sums of resistive currents at each node, $u(t) \in \mathfrak{R}^N$ is the vector of inputs, $v(t) \in \mathfrak{R}^N$ is the vector of node voltages, and N is the number of circuit nodes.

We are interested in the case in which the input signal $u(t)$ is quasiperiodic. We will say a signal is L -quasiperiodic if it can be written as a Fourier series with L fundamental frequencies. RF circuits are generally influenced by one periodic timing signal, often referred to as the LO or the clock, and one or more information signals. The fundamental assumption of the MFT method is that the circuit possesses a quasiperiodic steady-state response. That is, $v(t)$ is an $S+1$ quasiperiodic signal with fundamentals f_1, \dots, f_S, f_c , with f_c denoting the clock frequency. Furthermore, since all physical circuits have a finite bandwidth, $v(t)$ can be well approximated by taking only a finite number of terms in the Fourier series, so that

$$v(t) = \sum_{k_1=-K_1}^{K_1} \dots \sum_{k_S=-K_S}^{K_S} \sum_{k_c=-\infty}^{\infty} V(k_1, \dots, k_S, k_c) \times e^{-j2\pi k_1 f_1 t} \dots e^{-j2\pi k_S f_S t} e^{-j2\pi k_c f_c t}, \quad (1)$$

where $V(k_1, \dots, k_S, k_c) \in \mathbb{C}^N$. An interesting property of the MFT method is that it is not necessary to truncate to a finite number of harmonics of f_c , which is important since the clock typically causes most of the nonlinearity.

Now suppose that $v(t)$ is sampled at a discrete set of points $t'_n = t_0 + nT_c$, where $T_c = 1/f_c$ is the clock period, $t_0 \in [0, T_c)$ and n runs over the integers, to obtain a discrete signal $\bar{v}(t)$. Since

$$\bar{v}(t) = \sum_{k_1=-K_1}^{K_1} \dots \sum_{k_S=-K_S}^{K_S} \bar{V}(k_1, \dots, k_S) \times e^{-j2\pi k_1 f_1 t'_n} \dots e^{-j2\pi k_S f_S t'_n} \quad (2)$$

where $\bar{V}(k_1, \dots, k_S) = \sum_{k_c=-\infty}^{\infty} V(k_1, \dots, k_S, k_c) e^{-j2\pi k_c f_c t_0}$, the ‘‘envelope’’ $\bar{v}(t)$ is S -quasiperiodic and can be represented as a Fourier series in only the ‘‘information’’ fundamentals. The clock fundamental has disappeared. The continuous waveform is the waveform that has \bar{V} as its Fourier coefficients, or, equivalently, obtained by Fourier interpolation of the sampled points.

In principle, since there are only $K = \prod_{s=1}^S (2K_s + 1)$ Fourier coefficients to represent \bar{v} , once the value of K distinct points t_1, \dots, t_K along the sample envelope are known, the full envelope can be recovered. The envelope corresponding to the quasi-periodic operating point is obtained by obtaining K sample points that lie on the solution to the DAE given by (2).

Note that for each signal, the signal values, at the sample time points plus one clock cycle, $\bar{v}(t)$, is a delayed version of the signal values at the sample time points, i.e. there exists a linear operator D_{T_c} that relates \bar{v} and \bar{v}_c : $\bar{v}_c = D_{T_c} \bar{v}$ or $D_{T_c}^{-1} \bar{v}_c = \bar{v}$. Note that D_{T_c} is a real matrix and the relation holds for all signals, $n = 1, \dots, N$. It represents a boundary condition of (2).

To construct the matrix D_{T_c} , referred to as the delay matrix, consider the Fourier series of \bar{v} and \bar{v}_c . Referring to equation (2), we have

$$\bar{v}(t + T_c) = \sum_{k_1=-K_1}^{K_1} \dots \sum_{k_S=-K_S}^{K_S} \bar{V}(k_1, \dots, k_S) \times e^{-j2\pi k_1 f_1 t'_n} \dots e^{-j2\pi k_S f_S t'_n} \Omega_{T_c}(k_1, \dots, k_S) \quad (3)$$

where $\Omega_{T_c}(k_1, \dots, k_S) = e^{-j2\pi k_1 f_1 T_c} \dots e^{-j2\pi k_S f_S T_c}$. Thus if Γ is the matrix mapping sample points on the envelope to Fourier coefficients, then the delay matrix may be constructed as $D_{T_c} = \Gamma^{-1} \Omega_{T_c} \Gamma$. For more details, one can refer to [1].

3. EFFICIENT FINITE-DIFFERENCE METHOD

3.1 Discretization for large signal analysis

Given the circuit equation and the boundary condition in Section 2, we can discretize the equation using a finite difference scheme. Euler, trapezoidal, and Gear methods are the finite difference schemes commonly used in circuit simulators. For simplicity of presentation, we discuss the Euler method only, and we assume the grid of time steps is equally spaced.

First, we denote the inverse of the delay matrix as $D_{T_c}^{-1} = [d_{ij}]_{i,j=1,\dots,K}$. We assume $S = 1$ and $K = 2$ for simplicity in illustration, though the minimum number for K is 3 in our implementation ($K = 2 \times K_1 + 1 = 3$). The time steps in time interval 1 are denoted by $\bar{t}_0, \bar{t}_1, \dots, \bar{t}_M$ and those in time interval 2 by $\bar{\bar{t}}_0, \bar{\bar{t}}_1, \dots, \bar{\bar{t}}_M$. The discretized finite-difference equation takes the following form

$$\begin{bmatrix} \frac{1}{h} & & & -\frac{d_{11}}{h} & & -\frac{d_{12}}{h} \\ -\frac{1}{h} & \frac{1}{h} & & & & \\ & \dots & & & & \\ & & -\frac{1}{h} & \frac{1}{h} & & \\ & & & -\frac{d_{21}}{h} & \frac{1}{h} & -\frac{d_{22}}{h} \\ & & & & -\frac{1}{h} & \frac{1}{h} \\ & & & & & \dots \\ & & & & & & -\frac{1}{h} & \frac{1}{h} \end{bmatrix} \mathbf{Q} + \mathbf{I} + \mathbf{U} = 0 \quad (4)$$

where h is the uniform time step and \mathbf{Q} , \mathbf{I} , and \mathbf{U} are vectors of function values at grid points.

$$\mathbf{Q} = [Q(v(\bar{t}_1)), Q(v(\bar{t}_2)), \dots, Q(v(\bar{t}_M)), Q(v(\bar{\bar{t}}_1)), Q(v(\bar{\bar{t}}_2)), \dots, Q(v(\bar{\bar{t}}_M))]^T \quad (5)$$

and the same for \mathbf{I} and \mathbf{U} .

We employ Newton’s method to solve the discretized nonlinear circuit equation, Eq. (4). At iteration i , the Jacobian matrix is given

by

$$\begin{bmatrix} \frac{\bar{C}_1}{h} + \bar{\sigma}_1 & & & & -\frac{d_{11}\bar{C}_0}{h} & & & & -\frac{d_{12}\bar{C}_0}{h} \\ -\frac{\bar{C}_1}{h} & \frac{\bar{C}_2}{h} + \bar{\sigma}_2 & & & & & & & \\ & & \dots & & & & & & \\ & & & -\frac{\bar{C}_{M-1}}{h} & \frac{\bar{C}_M}{h} + \bar{\sigma}_M & & & & \\ & & & & -\frac{d_{21}\bar{C}_0}{h} & \frac{\bar{C}_1}{h} + \bar{\sigma}_1 & & & -\frac{d_{22}\bar{C}_0}{h} \\ & & & & & -\frac{\bar{C}_1}{h} & \frac{\bar{C}_2}{h} + \bar{\sigma}_2 & & \\ & & & & & & \dots & & \\ & & & & & & & -\frac{\bar{C}_{M-1}}{h} & \frac{\bar{C}_M}{h} + \bar{\sigma}_M \end{bmatrix}$$

where M is the number of time steps in each one of the two time intervals. Our method is matrix-implicit because we do not form the above matrix explicitly. Instead, we apply the GMRES method to solve the Jacobian system. A preconditioner is devised for the efficiency of the iterative solve.

3.2 Discretization for small signal analysis

We denote the solution of large signal by $v_{LS}(t)$. In small signal analyses, we assume

$$v(t) = v_{LS}(t) + \Delta v(t)$$

where $\Delta v(t)$ is orders of magnitude smaller than $v_{LS}(t)$ in amplitude. Consider a small signal source $\Delta u(t)$, we can write the circuit equation in the following form

$$\frac{d}{dt}Q(v_{LS} + \Delta v) + I(v_{LS} + \Delta v) + u + \Delta u = 0.$$

Since Δv is very small, the above equations can be written using a first-order Taylor series approximation:

$$\frac{d}{dt}Q(v_{LS}) + \frac{d}{dt}\left(\frac{\partial Q(v_{LS})}{\partial v_{LS}}\Delta v\right) + I(v_{LS}) + \frac{\partial I(v_{LS})}{\partial v_{LS}}\Delta v + u + \Delta u = 0.$$

Note that v_{LS} satisfies the circuit equation, we can reduce Eq. (3.2) to

$$\frac{d}{dt}\left(\frac{\partial Q(v_{LS})}{\partial v_{LS}}\Delta v\right) + \frac{\partial I(v_{LS})}{\partial v_{LS}}\Delta v + \Delta u = 0. \quad (6)$$

Assume that Eq. (6) is a linear quasi-periodically time-varying system. For periodic small signal stimulus, $\Delta u(t) = Ue^{j2\pi ft}$, the small signal response is quasi-periodic and is given by

$$v(t) = \sum_{k_1=-K_1}^{K_1} \dots \sum_{k_S=-K_S}^{K_S} \sum_{k_c=-\infty}^{\infty} V(k_1, \dots, k_S, k_c) \times e^{-j2\pi ft} e^{-j2\pi k_1 f_1 t} \dots e^{-j2\pi k_S f_S t} e^{-j2\pi k_c f_c t}. \quad (7)$$

In essence, we can view the small signal stimulus as yet another tone, $S+1$, in the large-signal analysis where we only retain the DC-term for this tone, i.e. $k_{S+1} = 0$. If we discretize Eq. (6) using backward Euler method with uniform time step, we arrive at a left-hand-side matrix similar to the Jacobian matrix in the large-signal case. The only difference is that $d_{ij}|_{i,j=1,2}$ need to be replaced by $\alpha \cdot d_{ij}|_{i,j=1,2}$ where $\alpha = e^{-j2\pi fTc}$.

3.3 Comparison of matrix-implicit approaches

Following the nested-GMRES preconditioning approach in [1], the outer preconditioner for solving the small-signal linear system chooses the capacitance and conductance matrices in one time interval to

represent the matrices in all time intervals. Here we chose those in the first time interval and transform the delay entries, d_{ij} 's, in place into the frequency domain. We obtain the following matrix

$$\begin{bmatrix} \frac{\bar{C}_1}{h} + \bar{\sigma}_1 & & & & -\frac{\omega_1 \bar{C}_0}{h} \alpha & & & & \\ -\frac{\bar{C}_1}{h} & \frac{\bar{C}_2}{h} + \bar{\sigma}_2 & & & & & & & \\ & & \dots & & & & & & \\ & & & -\frac{\bar{C}_{M-1}}{h} & \frac{\bar{C}_M}{h} + \bar{\sigma}_M & & & & \\ & & & & -\frac{d_{21}\bar{C}_0}{h} & \frac{\bar{C}_1}{h} + \bar{\sigma}_1 & & & -\frac{\omega_2 \bar{C}_0}{h} \alpha \\ & & & & & -\frac{\bar{C}_1}{h} & \frac{\bar{C}_2}{h} + \bar{\sigma}_2 & & \\ & & & & & & \dots & & \\ & & & & & & & -\frac{\bar{C}_{M-1}}{h} & \frac{\bar{C}_M}{h} + \bar{\sigma}_M \end{bmatrix}$$

where ω_1 and ω_2 are the eigenvalues of the inverse of the delay matrix which are complex numbers. This preconditioning system is block-diagonal and can be solved block-by-block. In each block, we have to apply an inner GMRES solver again for the preconditioning solve. The inner and final preconditioner in the inner GMRES is the block lower-triangular part of the above matrix which can be solved efficiently.

Note that in [1], Krylov-subspace recycling technique is applied in the inner GMRES solves in different blocks, which makes the solves more efficient. However, in different outer GMRES solves, we have to restart the inner Krylov-space recycling solves because the ‘‘random’’ change in the right-hand-side vector makes the Krylov-subspace reuse difficult for the new GMRES solve. Due to this reason, it is not effective to apply nested recycling GMRES solver in the quasi-periodic small signal analyses where one usually wants to solve many similar systems, with only α varying, for many frequencies. In this situation, one really wants to recycle the Krylov-subspace across different frequencies at the small-signal sweep level since the right-hand-side vector varies smoothly as the small-signal frequency changes, which leads to very efficient small-signal solves. Hence we need to have two levels of recycling if we want to apply the nested GMRES solver, one at the small-signal sweep level and one at the inner GMRES preconditioning solve level. The goal of recycling across small-signal frequencies is difficult to achieve if we need to restart the inner GMRES solves.

To facilitate Krylov-subspace reuse at the small-signal frequency sweep level which is very important for the efficiency of small signal analyses, we propose a different preconditioner for our quasi-periodic matrix-free approach. We simplify the preconditioning technique in [1] by eliminating one layer of GMRES solve. We apply the following preconditioner directly:

$$\begin{bmatrix} \frac{\bar{C}_1}{h} + \bar{\sigma}_1 & & & & & & & & \\ -\frac{\bar{C}_1}{h} & \frac{\bar{C}_2}{h} + \bar{\sigma}_2 & & & & & & & \\ & & \dots & & & & & & \\ & & & -\frac{\bar{C}_{M-1}}{h} & \frac{\bar{C}_M}{h} + \bar{\sigma}_M & & & & \\ & & & & & \frac{\bar{C}_1}{h} + \bar{\sigma}_1 & & & \\ & & & & & -\frac{\bar{C}_1}{h} & \frac{\bar{C}_2}{h} + \bar{\sigma}_2 & & \\ & & & & & & \dots & & \\ & & & & & & & -\frac{\bar{C}_{M-1}}{h} & \frac{\bar{C}_M}{h} + \bar{\sigma}_M \end{bmatrix}$$

Note that the capacitance and conductance matrices remain the

same in all the integration time intervals. This preconditioning method is similar to applying $D_{T_c} \otimes I_N$ to the shooting-method equation,

$$(D_{T_c} \otimes I_N) \bar{\mathbf{y}} - \Phi_{T_c}(\bar{\mathbf{y}}) = 0,$$

where Φ is the multi-cycle transition function from $t_k + 0$ to $t_k + T_c$.

In general, the condition number of the preconditioned system in the new approach is better than that in [1], because the new one does not approximate the capacitance and conductance matrices in all time intervals with those in one time interval. The new approach is also simpler and can be used successfully with the Krylov-subspace recycling technique at the frequency-sweep level in quasi-periodic small-signal analyses, which is verified in our numerical experiments.

3.4 Fourier spectrum calculation

In [1] two approaches for computing the Fourier spectrum was given. In both approaches, integration and DFT's are calculated in different steps. If the Fourier spectrum needs to be calculated for a large number of signals, i.e. N being large, the efficiency of these calculations can be significantly improved.

In the adjoint analysis in the quasi-periodic small signal analyses, one needs to modulate the small-signal stimulus vector with integration weights that transform quasi-periodic signals into quasi-periodic Fourier coefficients in one step. Note that in [1], quasi-periodic Fourier spectrum calculation is done in a few separate steps involving integration and multi-dimensional DFT's. A way to obtain the one-step Fourier integration weights has not been given.

Here we give a more efficient quasi-periodic Fourier spectrum calculation method. More importantly, the new approach gives an efficient way to calculate the one-step quasi-periodic Fourier integration weights. After we obtain these weights, one can calculate the weighted sums of any quasi-periodic signal efficiently. The weighted sums give us the quasi-periodic Fourier coefficients.

After convergence, the values $\bar{\mathbf{v}} = [v(t_1)^T, v(t_2)^T, \dots, v(t_K)^T]^T$ and the integration solution in $[t_i, t_i + T_c]$, $i = 1, \dots, K$ are available. Let

$$v(t) = \sum_{k_c=-K_c}^{K_c} \sum_{k_1=-K_1}^{K_1} \dots \sum_{k_S=-K_S}^{K_S} V(k_1, \dots, k_S, k_c) \times e^{-j2\pi k_1 f_1 t} \dots e^{-j2\pi k_S f_S t} e^{-j2\pi k_c f_c t}. \quad (3.1)$$

Define $\bar{\mathbf{v}}(\tau) = [v(t_1 + \tau)^T, v(t_2 + \tau)^T, \dots, v(t_K + \tau)^T]^T$. Then

$$\bar{\mathbf{v}}(\tau) = \bar{\Gamma}(0)^{-1} \bar{\Omega}(\tau) \begin{bmatrix} \vdots \\ \sum_{k_c=-K_c}^{K_c} V(k_1, \dots, k_S, k_c) e^{-j2\pi k_c f_c \tau} \\ \vdots \end{bmatrix}$$

and we assume $\sum_{i=1}^S k_i f_i$ corresponds to the p th sub-vector of the KN -vector (the actual correspondence is determined by the DFT). For a desired $V(k_1, \dots, k_S, k_c)$, two approaches for calculating the Fourier spectrum were given [1], one for the case where consistent time steps are used throughout K integration intervals and the other one for the case where time steps in different integration intervals are inconsistent. The total cost for the first approach is one KN -dimensional integration plus $(2K_c + 1)MN$ DFTs and the total cost for the second approach is $(2K_c + 1)K$ KN -dimensional integrations plus N DFTs which is more expensive.

In our new approach, the cost of one-time calculation of quasi-periodic integration weights for calculating the quasi-periodic Fourier

spectrum is only $O(KM + K^2)$. More importantly, it gives us the quasi-periodic Fourier integration weights needed in quasi-periodic small signal analyses. In calculating the quasi-periodic Fourier spectrum of the large signal operating point, one needs to calculate the integration weights only once. In subsequent quasi-periodic Fourier spectrum calculation, one just needs to multiply the solution with the appropriate weights and sum the results up to obtain the Fourier coefficient. The cost is only MN multiplications and MN additions for computing one Fourier coefficient, a speed-up of at least a factor of K .

It is easy to verify that for every E_p , a unit vector with $E_p(p) = 1$,

$$\begin{aligned} & \frac{1}{T_c} \int_0^{T_c} E_p^T \Omega(\tau)^{-1} \Gamma^{-1} \bar{\mathbf{v}}(\tau) e^{j2\pi k_c f_c \tau} d\tau \\ &= E_p^T \Gamma \left(\frac{1}{T_c} \int_0^{T_c} \bar{\mathbf{v}}(\tau) e^{j2\pi (\sum_{i=1}^S k_i f_i) \tau} e^{j2\pi k_c f_c \tau} d\tau \right). \end{aligned} \quad (3.2)$$

For simplicity, assume that $S = 1$ and $k_1 = 1$. Then we have three integration intervals. Now denote the plain integration weights in the three intervals as W^1, W^2 , and W^3 which are row vectors of size $1 \times M$, we can calculate the one-step integration weights with the following formula:

$$E_p^T \Gamma \begin{bmatrix} W^1 & 0 & 0 \\ 0 & W^2 & 0 \\ 0 & 0 & W^3 \end{bmatrix}. \quad (3.3)$$

We do not want to really calculate the multi-dimensional Fourier transformation for every column in the weight matrix. Rather we want to obtain the DFT matrix explicitly first. The multi-dimensional DFT matrix can always be obtained from applying the multi-dimensional DFT to unit vectors with negligible cost. Denote the matrix Γ as $[\gamma_{ij}]_{i,j=1,2,3}$, we have

$$E_p^T \Gamma \begin{bmatrix} W^1 & 0 & 0 \\ 0 & W^2 & 0 \\ 0 & 0 & W^3 \end{bmatrix} = E_p^T \begin{bmatrix} \gamma_{11} W^1 & \gamma_{12} W^2 & \gamma_{13} W^3 \\ \gamma_{21} W^1 & \gamma_{22} W^2 & \gamma_{23} W^3 \\ \gamma_{31} W^1 & \gamma_{32} W^2 & \gamma_{33} W^3 \end{bmatrix}. \quad (3.4)$$

The calculation of only one row in (3.4), specified by E_p^T , is necessary. For example, if $p = 3$, the one-step weights for quasi-periodic Fourier spectrum calculation in the three integration intervals are $\gamma_{31} W^1$, $\gamma_{32} W^2$, and $\gamma_{33} W^3$ respectively.

4. NUMERICAL RESULTS

In the first example, we apply finite difference method in obtaining the large-signal quasi-periodic operating point as a refinement step after shooting-Newton method. The test circuit in this example is a simple ideal multiplier that tests linear frequency-translation. In Fig. 1, one observes that the finite difference result is obviously better than the shooting result. Both methods use almost the same discretization. The difference is that in finite difference method we use the second-order Gear method at all the time steps while in shooting method we need to use backward Euler method initially to start the integration. Considering that frequency translation appears in almost all RF simulations, a finite-difference refinement after shooting method has converged appears to be worthwhile. We did an extensive comparison of finite difference method and shooting method on dozens of RF test circuits. We find that finite difference method improves the accuracy of shooting method in some cases and it never makes the shooting-Newton result less accurate.

Figure 1: Comparison of shooting and finite difference method results, signal after frequency-translation in one time interval.

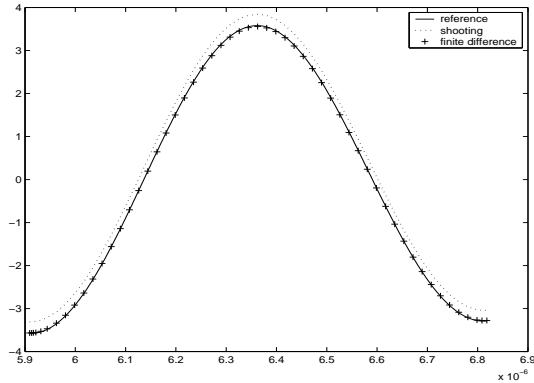


Table 1: Size of Krylov-subspace in quasi-periodic small signal (AC) analysis with frequency sweep.

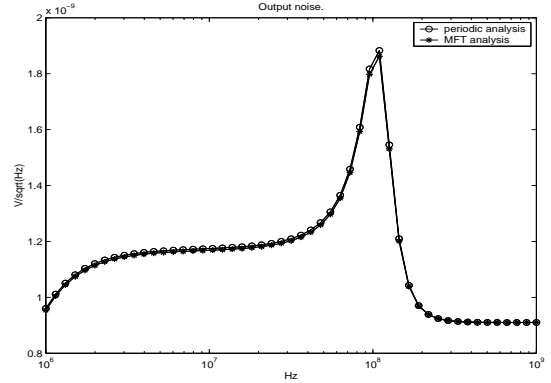
| Krylov-subspace size | K=3 | K=7 | K=15 |
|----------------------|-----|-----|------|
| 1 frequency swept | 76 | 109 | 114 |
| 51 frequencies swept | 105 | 130 | 135 |

In the second example, we show the effectiveness of the new preconditioner. The test circuit is a behavior-model receiver with two tones of frequency 1GHz and 910MHz respectively. A small-signal frequency sweep from 10MHz to 100MHz is done in the quasi-periodic analysis. In Table 1, it is shown that Krylov-subspace recycling technique works in our approach. After obtaining the Krylov-subspace in the GMRES solve at the first small-signal frequency, we only need to add less than one vector per solve in subsequent solves. One also observes that the number of GMRES iterations increases slowly with the number of time intervals, i.e. K , important for the success of MFT preconditioners. In our tests, the final size of the Krylov-subspace is independent of frequency points used in the sweep, which means that the more sweep frequencies the greater benefit of recycling.

In the third example, we present quasi-periodic noise analysis results. The test circuit is a transistor-level mixer. We set one tone at 1.8GHz operating frequency and the other tone at 0.9GHz frequency such that we can run both periodic noise analysis and quasi-periodic noise analysis without any difficulty. We compare the output noise results obtained by the two analyses. From Fig. 2 we can see that the results agree with each other, which verifies the correctness of the new method.

In the last example, a high-performance image rejection receiver, discussed in [6] is simulated to obtain quasi-periodic noise results. The circuit was driven by a 780MHz LO and two 50mV closely placed RF inputs, at 840MHz and $840\text{MHz}+10\text{KHz}$, respectively. Three harmonics were used to model each of the RF signals. To understand the efficiency of the quasi-periodic MFT noise analysis method, consider that periodic noise analysis would need to put the fundamental frequency at 10kHz and need about a million time steps and billions of unknowns to obtain the periodic operating point. The number of matrix-vector products in quasi-periodic steady-state analysis using the shooting method, without the GMRES recycling in the inner GMRES solver, is 50 while the number of matrix-vector products in the finite difference method is only 16.

Figure 2: Comparison of periodic and quasi-periodic analyses output noise results.



5. CONCLUSIONS

In this paper we presented a finite-difference approach to quasi-periodic steady-state analysis using the MFT method. We also discussed the small signal analyses that are performed by linearizing around the quasi-periodic steady-state. An efficient iterative solver, used successfully with Krylov-subspace recycling technique, was presented. An efficient way for calculating the quasi-periodic Fourier integration weights was also given.

6. ADDITIONAL AUTHORS

Additional authors: Joel Phillips (Cadence Berkeley Laboratories, e-mail: jrp), Keith Nabors (Cadence, e-mail: nabors) and Kenneth Kundert (Cadence, e-mail: kundert@cadence.com).

7. REFERENCES

- [1] D. Feng, J. Phillips, K. Nabors, K. Kundert and J. White, Efficient computation of quasi-periodic circuit operating conditions using a mixed frequency/time approach, Proc. 36th Design Automation Conference, New Orleans, LA, June, 1999.
- [2] B. Yang and J. Phillips, A multi-interval Chebyshev collocation method for efficient high-accuracy RF circuit simulation, to appear in Proc. 36th Design Automation Conference, 2000.
- [3] J. Roychowdhury and D. Long and P. Feldmann, Cyclostationary noise analysis of large RF circuits with multitone excitations, IEEE J. Sol. St. Circuits, vol. 33, pp. 324-336, 1998.
- [4] D. Feng, unpublished.
- [5] R. Melville and P. Feldmann and J. Roychowdhury, Efficient multi-tone distortion analysis of analog integrated circuits, Proc. Custom Integrated Circuits Conference, May, 1995.
- [6] R. Telichevesky and J. White and K. Kundert, Receiver characterization using periodic small-signal analysis, Proceedings of the Custom Integrated Circuits Conference, May, 1996.
- [7] J. Roychowdhury, Efficient methods for simulating highly nonlinear multirate circuits, Proc. 34th Design Automation Conference, Anaheim, CA, June, 1997.